Connection of Steel Beams to Concrete-Filled Tubular Columns

Hassan SHAKIR-KHALIL
Division of Civil Engineering
University of Manchester
Manchester, England
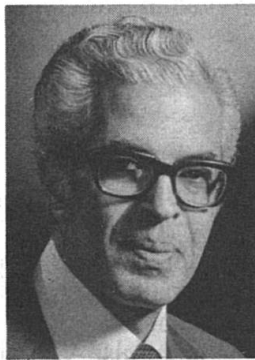
Hassan Shakir-Khalil received
his BSc and MSc degrees in Civil
Engineering from the University
of Cairo, Egypt. He obtained his
PhD degree from the University of
Cambridge, England, UK. He has been
researching in the field of concrete-filled
tubular columns for the last 15 years.

Summary

Tests have been carried out on 36 full scale beam-to-column connections. The connections
were manufactured by connecting steel beams to concrete-filled tubular columns through
either finplate or T-cleat connections. The columns used were either circular or rectangular
(CHS & RHS) hollow steel sections. Except for the last eight specimens, all the other test
specimens were symmetrically loaded.

Experimental Work and Numerical Analysis

Table 1 gives a summary of all 36 specimens tested in this experimental investigation. The
column tubing of all specimens is 2.8m long, and the column lengths have 15mm thick end
plates. The side beams connected to the test specimens of series A-E were symmetrically
loaded. However, the eight specimens of series 'F' had either one side beam, or their side
beams were unsymmetrically loaded. The webs of the side beams of series A-D were bolted
to 10mm thick finplates which had been welded to the columns. Finplates were replaced by
T-cleats in series E&F as a result of the large out-of-plane deformations of the RHS walls to
which the finplates were welded. Both types of connections are shown in Fig 1.

Figure 2 shows a schematic view of the test rig and test specimen. The rig consists of a base
and an upper cross-head connected together by four vertical ties of steel hollow section. The
rig is self contained, and the base is securely bolted to the laboratory strong floor. The rig
has a head room of about 3m. The loads applied to the side beams by the hydraulic jacks are
transferred to the beams through a platform and load cells. The loading platform was used in
order to maintain the location of the jacks and at the same time to be able to apply the beam
loads at any required eccentricity by simply moving the load cells to the new locations. The
beam loads were applied at varied distances from the centre of the column. The beam and
column loads, P_2 and P_1, were increased proportionately, and the beam-to-column load ratio
was mainly taken either 1:8 or 1:5.

The rig was originally designed for testing the symmetrically loaded specimens of series A-E,
and was thus provided with no lateral bracing. A triangulated, stiff in-plane bracing, not
shown in Fig. 2, was therefore welded between the vertical ties in order to ensure the lateral
stability of the test rig before testing the unsymmetrically loaded beam-to-column connections
of test series F. During the test procedure, all specimens were also laterally restrained at mid-
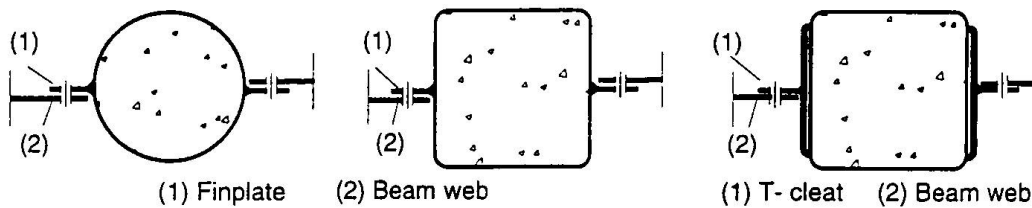
Fig.1 Finplate and T-Cleat Connections

height as shown by '7' in Fig. 2. This lateral restraint was connected at its other end to a stiff bracing system which was securely connected to the strong floor.

The test specimens were provided with electric resistance strain gauges and displacement transducers. The displacements were measured in the plane of loading and also transverse to the loading plane. Displacement transducers were also placed against the column end plates to record the column shortening and end rotations. The strain measurements were carried out over distances equal to three times and twice the lateral dimension of the steel hollow section above and below the finplate/T-cleat positions respectively, an arrangement that was found to be satisfactory.

The ABAQUS software package was used to model the test specimens of series 'F'. It can be seen from the numerical model shown in Fig. 3, that the side beams were not modelled, and neither were the bolt holes in the connection. The T-cleat stem was extended to model the beam, and the numerical model was only used to

Series	Column Size	Type of Connect.	No. of Spec.	Connect. Loading
A	168.3x5CHS	Finplate	8	$e2=e1$
B	150x150x5RHS	,,	8	,,
C	219.1x6.3CHS	,,	2	,,
D	200x200x6.3RHS	,,	2	,,
E	150x150x5RHS	T-Cleat	8	,,
FI	150x150x5RHS	,,	4	$e2=0.0$
FII	150x150x5RHS	,,	4	$e2<e1$

Table 1 Sumary of Test Series

1. Cross head
2. Ties (Four)
3. Jack + Load Cell
4. Base
5. Concrete-filled tube
6. Side beam
7. Lateral bracing

Fig.2 Test Rig and Specimen   Fig.3 Num. Model

predict the overall column failure. The boundary conditions at the top of the numerical model were similar to the experimental end conditions in which the top end of the column was fixed in position, and was allowed to rotate freely only in the plane of loading. However, the central nodes at the lower end of the model, and also at its mid-height, were allowed to move vertically, thus allowing for column shortening.
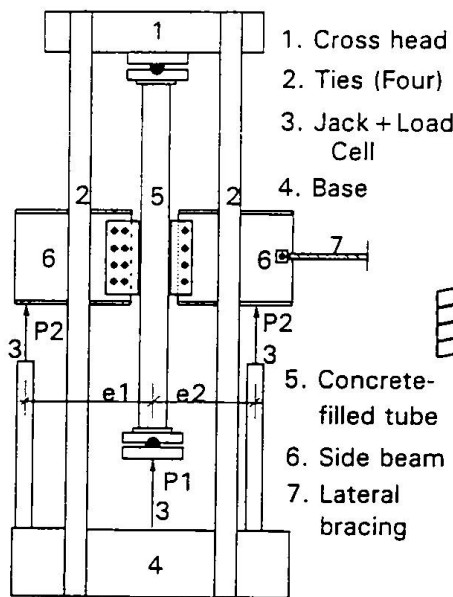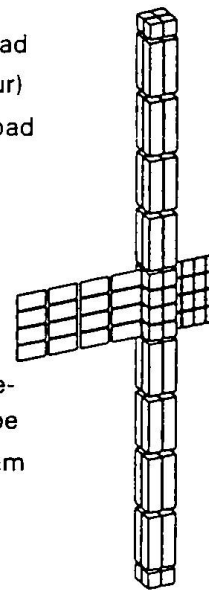
The numerical model has 48 concrete brick elements (C3D20), 96 steel shell elements (S8R) for the RHS steel tube, 16 steel shell elements (S8R) for the T-cleat flanges, 32 steel shell elements (S8R) for the T-cleat stems and 8 rigid brick elements (C3D20) for the end loading plates. In all, the model has 200 elements and 1081 nodes.

Column-Pile Joints Made of Steel Pipes Filled with Concrete

Hideaki TAKANO
Civil Engineer
Company Joshin-etsu
Takasaki, Japan

Hideaki Takano born 1955,
Complete the Department of
Junior College Nihon University.

Summary

For a connection of a column and pile made of concrete-filled steel pipes with different diameters, a simple overlap joint in which a smaller diameter pipe is inserted by the specific length to a larger diameter pipe with concrete filled between them has been proposed as an economical and effective joint system. The experiments indicate that the method to predict ultimate loads of the present joints has been proposed.

1. Test Program

As illustrated in Fig.1, cantilevers of concrete-filled steel pipes (CFSPs) having the present overlap joints are loaded at the top of the column.

2. Proposed Model for Prediction of Ultimate Load

Judging from the failure processes of the present joints, it is considered that the bending moment and shear force applied to the column are carried by the couple forces of horizontal bearing pressure and friction developed on the embedded part of the column. Therefore, the authors try to predict the ultimate load of the joints by assuming a load-carrying model illustrated in Fig.2, based on experimental observations of the present tests and finite element analyses previously carried out.

2.1 Balance of moment

From the balance of the moment shown in Fig. 2,

$$M - T\left(\frac{2\sqrt{2}}{\pi}\right)d = -\frac{LP^2}{3(2P-Q)} + (P-Q)\frac{L(5P-2Q)}{3(2P-Q)} \quad \text{(1)}$$

where M and Q are bending moment and shear force applied to the column respectively, and P and T are resultant forces of bearing pressure and frictional stresses developed on the column respectively. In the above equation, the friction is assumed to be developed on one-forth the circumference of column on tensile and compressive sides respectively.

2.2 Frictional force at ultimate states

The frictional stresses developed between the column pipe and the concrete filled are assumed to be subject to Coulomb's friction criteria. That is;

$$\tau_{max} = c + \sigma_n \tan\phi \quad \text{(2)}$$

τ_{max} : maximum frictional stresses σ_n : normal stresses at the interface

c : cohesion of friction ϕ : friction angle

Then, a resultant force of frictional stresses T is described as follows;

$$T = c\frac{\pi}{4}dL\frac{P-Q}{2P-Q} + \frac{\pi}{2\sqrt{2}}(P-Q)\tan\phi \quad \text{(3)}$$

2.3 Bearing pressure at ultimate states

The bearing pressure developed on the column is assumed to be determined by shear capacities of the shear panels which consist of the pile pipe and annular concrete in the overlapped part with the length of L. Therefore, the bearing pressure is described as follows;

$$P = V_s + V_c \qquad (4)$$

where V_s is a shear capacity carried by steel pipe and V_c is a shear capacity carried by annular concrete.

The shear capacity of the pile pipe is to be calculated as follows;

When the couple force of bearing pressure is applied to the pile pipe, the tensile force band with the width of 2/3L is assumed to be formed on the lateral panel of the pile pipe in the direction from the center of action of the total bearing pressure on the compressive side to that on the tensile side. At the ultimate states, the tensile force band yields in full. Then,

Fig.1 Description of Test

$$V_s = f_y \cdot 2t \cdot \frac{D'}{\sqrt{\left(\frac{2}{3}L\right)^2 + D'^2}} \left(\frac{2}{3}L\right) \qquad (5) \qquad \text{where} \quad D' = \frac{\pi}{4}D$$

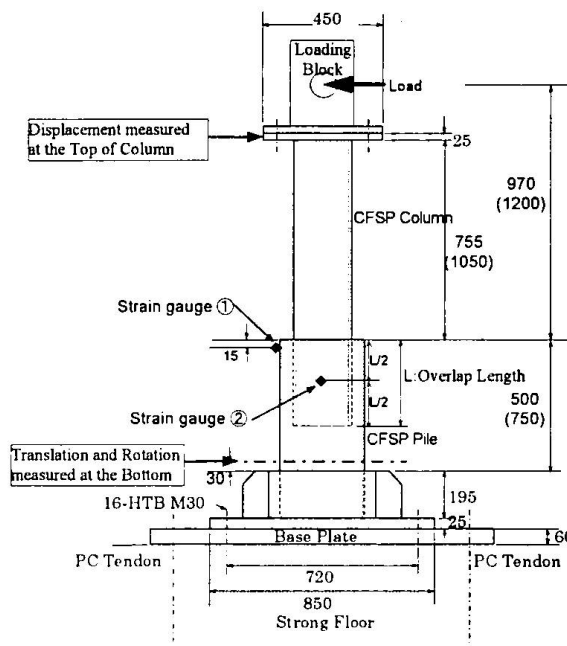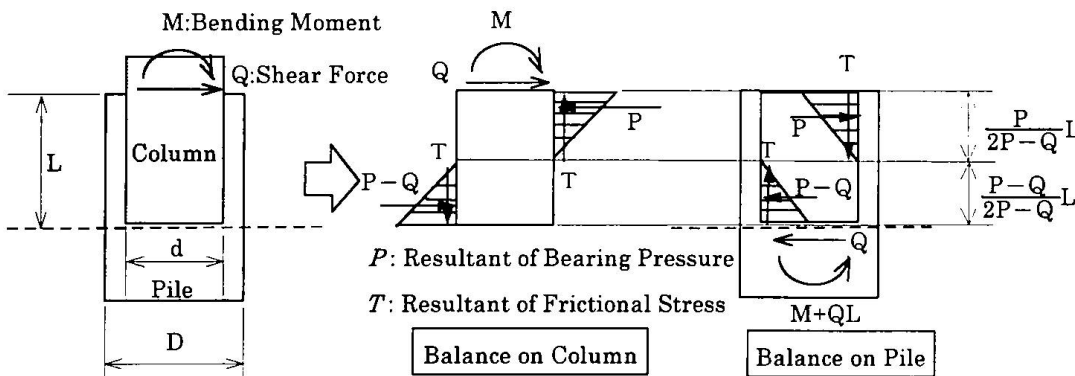Fig. 2 Load Carrying Model for Predicting Ultimate Loads

On the other hand, because in the experiment the annular concrete was pulled out of the pile pipe, the shear capacity carried by the annular concrete is determined by the resisting force which prevents the concrete from being pulled out.
Therefore, the shear capacity V_c is;

$$V_c = \frac{3\sqrt{2}}{\pi} \frac{D}{L} \left\{ \frac{\pi}{4} D \cdot \left[L - (D-d)/2 \right] \cdot c - \frac{\pi}{4} d \frac{L}{2} c \right\} \qquad (6)$$

Consequently, the ultimate load can be calculated by solving equation (1) after substituting (3), (4) ,(5) and (6) into (1).

The calculation yields a satisfactory good approximation to the experimental ultimate loads, though some underestimation occurs.

Behaviour of the Composite Beam-to-Steel H Column Connection

Akira MATSUO
Dr. Eng.
Hiroshima Univ.
Higashi-Hiroshima, Japan

Yuji NAKAMURA
Ph.D.
Hiroshima Univ.
Higashi-Hiroshima, Japan

Rafeek W. SALIB
Dr. Eng.
Suez Canal Univ.
Port Said, Egypt

Yoshimasa MATSUI
Dr. Eng., Civil Engineer
Keisoku Research Consultant
Hiroshima, Japan

Summary

The main purposes of this paper are to know the behavior of the composite beam-to-steel H column connection and to give the shear yielding and maximum strengths and panel moment $_pM$- shear deformation γ relation. The maximum strength is formulated through limit analysis. The panel moment - shear deformation relation is formulated considering the Bauschinger effect and the isotropic and kinematic hardening rule.

1. Introduction

It is well known that a concrete slab connected to a steel beam increases the stiffness and strength of the beam. It is also presumable that the concrete slab increases the shear stiffness and strength of the beam-to-column connection. The shear strength and the panel moment $_pM$- shear deformation γ relation of bare steel beam-to-column connections are presented(Matsuo,1995). However, the yield strength of the panel with a concrete slab is 20 to 40% larger than the bare steel connection(Nakao,1984). This paper presents the experimental results and the formulation of the shear strengths and $_pM$- γ relation considering the effects of the concrete slab.

2. Experimental Plan and Results

The experimental parameters are the shapes(X-type, T-type of frames), member strength(weak beam, weak column), the ratio of the panel yield strength to other members($R_{py} \fallingdotseq 0,0.5,0.7$), aspect ratio($H_b/H_c$=1.0,1.5) and displacement ratio(δ^-/δ^+=1.0,1.2). δ^- and δ^+ are the displacements of the loading points of the negative and positive bending beams. For example, the specimen X10B45-10 indicates X-type, H_b/H_c=1.0, weak beam, R_{py}=0.45 and δ^-/δ^+=1.0. Experimental results of the 13 specimens are listed in Tab.1, where $_pM_{yc}$ and $_pM_{uc}$ are the experimental yield and maximum panel strengths respectively. An experimental $_pM$- γ relation is shown in Fig.1

3. Analytical Strength and $_pM$- γ Model of the Panel

Analytical yield strength $_pM_{yc}$ is obtrained by Eq.1 following to Nakao(1987). M_{b1}, M_{b2}, Q_c and V_R are negative and positive face moment in the beam, column shear force and an effective volume of the panel. $_pM_{yc}$ predicts the experimental $_pM_{yc}$ fairly well in Tab.1. It is well known that the load carrying capacity of the panel increases after yielding, which is caused by strain hardening effect of the steel plate and direct transmission $_FM$ of the bending moment from the beam to column through 4 corners of the panel and concrete slab. Changing each parameter in Eqs.2 the ultimate strength of $_FM$ is given as the minimum value of $_FM^+ + _FM^-$ (Eqs.2) which is derived from the plastic deformations illustrated in Fig.2. In Eqs.2 L_c, L_b, σ_{yw} and t_{wb} are the lengths of the column and beam, the yield stress and thickness of the beam web. As an approximate value $_FM^+ = _FM^- + C_u d'$ is also given by neglecting the axial deformations of the beam flanges(n=0). The total strength of the connection is given by Eq.3. The panel strength when the concrete slab is crashed is given by $(\tau_y + \tau_u)V_p/2$, as the crash of the concrete slab started at an early stage. The compressive strength C_u of the concrete at the face of the column flange is obtained as follows.

Eqs.2 and 3 are first applied to the specimens which have no panel plate and $1.4F_c A_c$ is found as the most appropriate value of C_u, where F_c and A_c are the compressive strength of concrete and the area of the flange in contact with the slab. This C_u is also used for the other cases where the connection has the panel plate. In Tab.1 $_pM_{uc1}$ and $_pM_{uc2}$ correspond to the maximum strengths calculated, considering and neglecting the axial deformation e of the beam flanges. Both $_pM_{uc1}$ and $_pM_{uc2}$ predict the experimental strength well. Judging from Eq.3 in case of n=0 the resisting panel moment corresponding to the current shear deformation γ consists of τV_p, $_FM_s$ and Cd', where τ, $_FM_s$ and C are the resisting shear stress of the panel, the bending moment transmitted through the 4 corners of the panel and the compressive force of the slab corresponding to γ. $_pM$-γ relations are formulated as follows. τV_p-γ and $_FM_s$-γ relations are seperately formulated as two springs connected in series. Each spring is given as a bi-linear type and satisfies the isotropic and kinematic hardening rule (Tsuji,1988). The compressive force C to the contraction Δ (=γd') relation of the slab is followed to Shiga(1988). Predicted $_pM$-γ relation is shown in Fig.1.

$$\tau = [\, M_{b1} + M_{b2}\, H_b /(H_b + d') - Q_c H_b\,]\, /\, V_p \tag{1}$$

$$_FM^- = 2\,S\,a\,(a+b-c)^2 /b + 2\,(1+a/b)(M_{ubf} + M_{ucf}) + 2\,a\,(M_{pbf} + M_{pcf})/b \tag{2a}$$

$$_FM^+ = [\,(S\,a\,(a+b-c)^2\,(2+k_2(2-H_b\,/\,2a))/b + M_{ubf}\,k_2 Z(2+(nN_{ubf}\,/\,2M_{ubf})^2\,(1+((H_b+Z)/Z)^2\,))\,/n$$
$$+ 2M_{pbf}\,a(1+k_2)/b + M_{ucf}(2k_1+(2k_1-H_b/b)k_2) + M_{pcf}\,a(2+k_2(2-H_b/a))/b + C_u((-Z+d')k_2+d')\,]$$
$$/\,(1+k_2(1-H_c/L_b)/k_3\,) \tag{2b}$$

where $k_1 = 1+a/b$, $k_2 = k_1 n/(Z-k_1 n)$, $k_3 = 1-H_b/L_c-H_c/L_b$, n= eZ/(Hb+Z)θ and S=$\sigma_{yw} t_{wb}$

$$_pM_u = (\tau_y + \tau_u)\,V_p/2 + _FM^+ + _FM^- \tag{3}$$

REFERENCES
1)Nakao M.: Annual conference of AIJ, (1982) 1869-1870, (1983) 1259-1260, (1984) 1565-1566, (1987) 905-906 2)Matsuo A.: IABSE Symposium San Fransisco, (1995) 1435-1440 3)Tsuji B.: Transactions of AIJ, No.270 (1978) 17-22, 4)Inoue K.: Annual conference of AIJ, (1995) 523-524, 5)Shiga T.: Annual conference of AIJ, (1986) 377-378

Tab.1 Experimental and analytical results (unit:tmm)

| Specimens	pMye	pMyc	pMyc/pMye	pMue	pMuc1	pMuc1/pMue	pMuc2	pMuc1/pMue
X10B45-10	7167	7116	0.993	12021	13221	1.100	12170	1.012
X10B45-12	6333	6944	1.096	12839	13465	1.048	12293	0.957
X10B67-12	10850	10748	0.991	17257	17608	1.020	16436	0.952
X10B00-10	-	-	-	5822	6965	1.196	5914	1.016
X10B00-12M	-	-	-	5662	7209	1.273	6037	1.066
X15C33-10	9800	9724	0.992	18872	17725	0.939	16522	0.875
X15C33-12	9200	9338	1.015	18710	17725	0.947	16522	0.883
X15C66-10	18667	20244	1.084	31030	28762	0.927	27559	0.888
X15C00-10	-	-	-	6600	8292	1.256	7089	1.074
X15C00-10M	-	-	-	6642	8292	1.248	7089	1.067
T15B59	8850	8781	0.992	15602	17092	1.096	15658	1.004
T15B77	11700	11905	1.018	20618	21030	1.020	19596	0.950
T15B00	-	-	-	6259	7659	1.224	6225	0.996
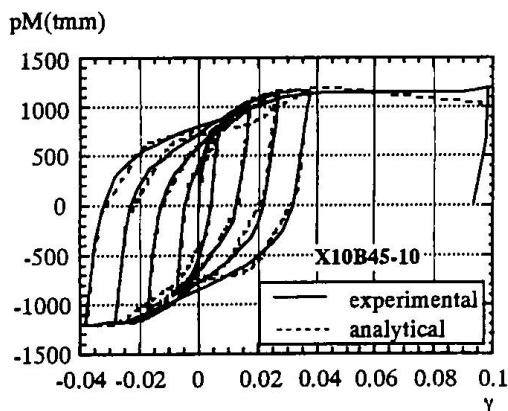
Fig.1 pM- γ relation of panel
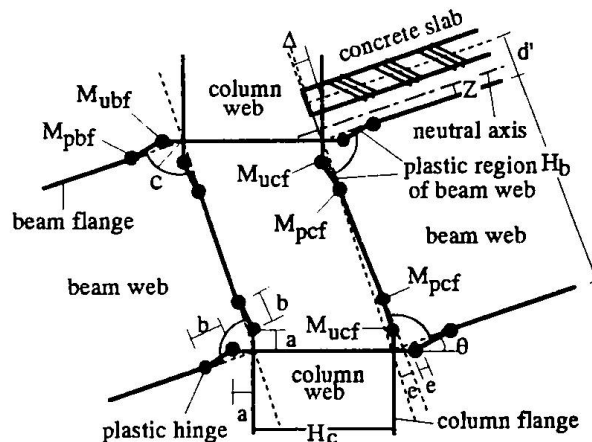
Fig.2 Plastic deformation of the connection

Composite Rahmen Railway Viaduct of PPC Beam and Steel Box Beam

Harumi TABATA
Assistant Manager
East Japan Railway Co.
Tokyo, Japan

Tadayoshi ISHIBASHI
Dr. Engineer
East Japan Railway Co.
Tokyo, Japan

Norio KAMATA
Deputy Manager
East Japan Railway Co.
Tokyo, Japan

Yasuaki HOSOKAWA
Assistant Manager
East Japan Railway Co.
Tokyo, Japan

Summary

The railway viaduct required aesthetic improvements, as the space under the bridge was to be used as a footpath, so it was required to reduce both the number of pillars on this viaduct and, further, to reduce the diameter of the pillars. Consequently, the beams were basically constructed in the form of a PPC box-type, and at places where the bridge is long, the structure fashioned as a steel box beam. The piers were made of steel pipe wound RC pillars. In order to increase the bridge's anti-earthquake properties, the structure was converted to a complex Rahmen viaduct which is unified between these 2 types of beams and piers. This report describes the materials and design of these connectors.

1. Circumstances

At the time of Nagano Winter Olympic Games in 1998, the Hokuriku Super Express will be extended to Tokyo Station. To accommodate this extension, a railway viaduct on the Chuo-Line (about 970 m in length) is to be constructed. This viaduct was constructed taking into considerations the scenery surrounding the Tokyo Station which is noteworthy as the gateway of Japan (Figure-1).

2. Whole structure

The pillars of this viaduct were made of reinforced concrete (RC) on the railway side and steel pipe wound RC on the road side, making the shape on each side very different (Figure-2). If a pier is made into a single gate-type structure, when a large sideways horizontal force is applied such as in the case of an earthquake, because of the difference in displacement in the upper end of the pier, a large distortion occurs in the pier. For this reason, the entire viaduct was made into a Rahmen structure of multiple lengths, and the rigidity of the entire body (against plane distortion) was increased.

3. Connection of beam and pier

As for the structural form of the upper area, the general parts were made of PPC beam, but the parts of the crossing over the road were made of steel box beam because the length of bridge was relatively long (39 m.) The viaduct was in the form of a complex Rahmen structure which unified 2 types of beams as well as the crossbeams of the piers. The connecting part of the beam and the pier is shown in Figure-3. The design of the connecting part was made so as to secure an adequate

safety ratio (F=1.0) against the destruction of the cross section material, and to prevent stretching stress at the time of active load effects, considering the influence of temperature. As an example of PC cable arranged to this connecting part, there is a 12E15.2×6 set at the upper position of original point.

Figure-1   Viaduct completion forecast picture
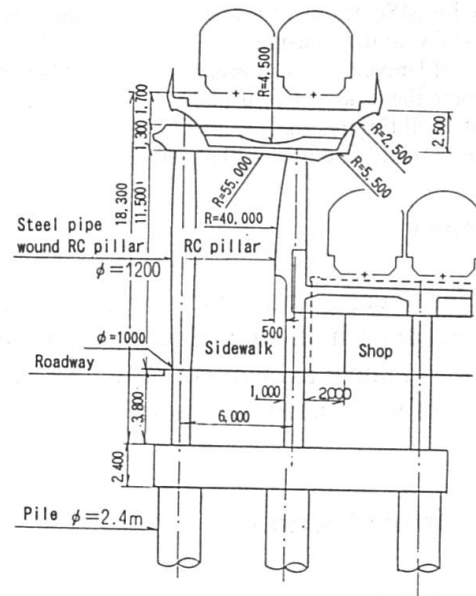

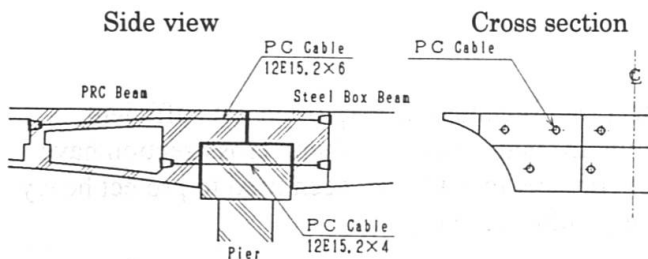*Figure-2   Cross section of viaduct*
(unit:mm)

Figure-3   Connecting parts between beam and pier

4.   Connections between steel pipe wound RC pillars and footings

As shown in Figure 1, the pillars of the viaduct on the left side were planned between the road and the footpath. Therefore, the pillar was to be made as thin as possible in order not to obstruct the passage of pedestrians. To cope with these demands, and considering the scenery, the pillars were made to a diameter of 1.0 meter on both ends and 1.2 meters in the center in the shape of an entasis (shaped like a cigar.) As for the constitution of the cross-sections of the pillars, steel pipes were used as Stirrup, and steel pipe wound RC pillar were constructed so as to allot the stretching forces to the iron bars in the concrete. In order to decide the arrangement of the iron bars at the connecting part of the upper crossway beam and steel pipe wound RC, experiments in horizontal load changing, using a 1/3-size model; results were applied to the actual design.

5.   Postscript

Investigations were made in accordance with the above descriptions; the particular nature of each structure was determined, and the structure was erected. This viaduct was completed in November, 1996, and the train is currently in operation. The Hokuriku Super Express will begin operation starting in Autumn, 1997.

Punching Failure Mechanism of Composite Slab-Column Joints

Andrzej B. AJDUKIEWICZ
Professor in Struct. Eng.
Silesian University
Gliwice, Poland

Alina T. KLISZCZEWICZ
Assistant Professor, PhD, CE
Silesian University
Gliwice, Poland

Jacek S. HULIMKA
Assistant, MSc, CE
Silesian University
Gliwice, Poland

He got his MSc degree (1961) and
PhD (1968) at the Silesian
Technical University. At present
he is there the head of Department
of Structural Engineering. Author
of several books and over 130 papers.

She was graduated in 1972 and got
her PhD in 1984 from STU. The
author of over 60 papers and
the leader of research projects.

He got his MSc degree in 1987
from STU. Involved in
experimental research on concrete
structures.

Summary

The idea of composite joints in slab-column skeletal structures deals with introduction of precast members from high-strength concrete as combined head-and-column elements. As behaviour of such joints under axial or eccentric loads has not been clarified, therefore the series of full-scale models of joints have been tested up to failure to obtain basic data about the failure mechanism.

1.   Introduction

The carrying capacity of flat-plates without shear reinforcement is very often not sufficient, particularly at interior column supports. Recently, in such cases the column cross-section have been enlarged or the special shear reinforcement or steel inserts have been used to protect heavy stressed support zones against the rapid punching failure (see [1]).

On the other side, the tests of monolithic slab-column joints indicated the significant role of compressive strength and deformability of concrete in slab around the column face, where biaxial compression was stated [2]. Therefore, application of high-strength concrete should be considered as the simplest method of the zone strengthening [3],[4]. The idea of composite structure with precast head-and-column elements from HSC (e.g. C70 or C80) and the remaining parts of slab from ordinary concrete was proposed in the first row for simple multi-storey buildings, like car-parks [5]. At least two benefits in such buildings are expected: the support zones strong enough without additional shear reinforcement and reduction of column sections.

To introduce the idea into the practice some designers' doubts should be clarified. The behaviour of such joints up to failure as well as carrying capacity of joints must be tested on full-scale models (to omit the size effects). Synthesis of observations from the tests of first series of six models are presented in this paper.

2.   Test Observations

In monolithic joints (Fig.1a) axisymmetrically loaded up to punching failure the shape of failure surfaces are always observed as truncated cones. The inclination α of basic crack depends mainly on the flexural reinforcement ratio and oscillate from 25^0 to 35^0.

In composite joints, in which the difference in concrete strength in members was not significant and both concretes were from the range of normal-strength concrete (e.g. C30 in head and C15 in slab) the behaviour at failure was very similar to that in monolithic joints (Fig.1b). The difference in failure crack was small: angle $\alpha \cong \beta$ from 32^0 to 36^0.

Quite different situation was recorded in tests of models with relatively strong heads - precast parts from concrete about C70 and monolithic slab from ordinary concrete C15. The failure was observed in two phases. The main top crack in slab occurred earlier at about 60% of ultimate load as a first phase of punching. The second phase was observed as sudden, noisy crack at the maximum recorded load. After cutting reinforcement the failure surface in the shape of double truncated cone was uncovered (Fig.1c). The angle α was from 40^0 to 48^0, while the angle β was from 19^0 to 21^0. The value of ultimate punching load in this case was about 10% greater than that in case presented in Fig.1b, at the same ratio of flexural reinforcement in both cases.
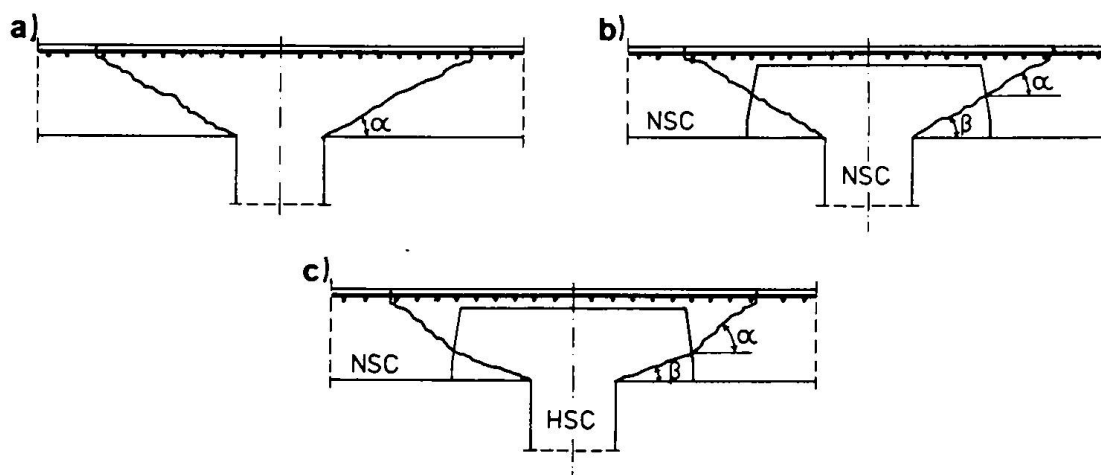

Fig.1. Recorded shapes of failure surface in axisymmetrical punching shear of models

3. Conclusions

The behaviour of composite slab-column joints with HSC head-and-column members was observed significantly different from that known from monolithic joints. The two-phase failure of such composite joints was recognized as more advantageous due to the warning signal than the increment in the final punching resistance.

References

[1]   Ajdukiewicz A., Starosolski W.: *Reinforced-Concrete Slab-Column Structures*. Elsevier, Amsterdam-Oxford-New York-Tokyo, 1990, p.XXIV+372.

[2]   Broms C.E.: *Punching of Flat Plates - A Question of Concrete Properties in Biaxial Compression and Size Effect*. ACI Structural Journal, V.87, No 3, 1990, pp.292-304.

[3]   Ajdukiewicz A.,Kliszczewicz A.: *Application of High-Strength Concrete in Composite Skeletal Structures*.Third Int. Symposium on *Utilization of High Strength Concrete*, Lillehammer, 20-24 June 1993, pp.449-456.

[4]   Hallgren M.: *Punching Shear Capacity of Reinforced High Strength Concrete Slabs*. Doct.Thesis. The Royal Institute of Technology, Stockholm, 1996, p.206.

[5]   Ajdukiewicz A., Kliszczewicz A.: *Simple Construction of Composite Slab-Column Structures*. Proc. of 15th IABSE Congress, 16-20 June 1996, Copenhagen, pp.589-584.